STRUCTURAL AND MAGNETIC PROPERTIES OF $MgFe_2O_4$ FERRITE NANOPARTICLES SYNTHESIS THROUGH AUTO COMBUSTION TECHNIQUE

Harshal B. Desai,[a] Arun Kumar[b] and Ashish R. Tanna[a]*

Keywords: Ferrite nanoparticles; auto combustion method; X-ray diffraction; vibrating sample magnetometry; Mossbauer spectroscopy.

Magnetic magnesium ferrite nanoparticles have been synthesized through an auto combustion method. The prepared ferrite is characterized by X-ray diffraction, particle size analyzer, Fourier transform infrared spectroscopy, scanning electron microscopy, energy dispersive X-ray spectroscopy, vibrating sample magnetometry and Mossbauer spectroscopy. It is confirmed that the prepared sample has a cubic structure in nature through XRD. The crystalline size is determined by the Debye Scherrer formula, results are confirmed with particle size analyzer data. The FTIR spectra are used to calculate the force constant of tetrahedral sites and octahedral sites. The morphology and the quantitative analysis of the synthesized sample are studied by SEM and EDAX. The prepared nanoparticles' magnetic properties have been studied at room temperature by means of hysteresis loop measurement using vibrating sample magnetometer and Mossbauer spectroscopy. The value of saturation magnetization, coercive field, and cation distribution of magnesium ferrite is obtained from the magnetic measurements.

*Corresponding Authors
E-Mail: ashish.tanna@rku.ac.in
[a] Department of Physics, School of Science, RK University, Rajkot-360020
[b] Department of Physics, Kurukshetra University, Kurukshetra, Haryana-136119, India

INTRODUCTION

The spinel structure is a cubic crystal system constructed of 32 closely packed oxygen atoms with 64 tetrahedral sites and 32 octahedral sites. The electrical neutrality in spinel ferrite is maintained by $(M^{2+})[Fe^{3+}]_2O_4$ where M^{2+} (A sites) is situated at 8 tetrahedral sites and Fe^{3+} (B sites) is situated at in and 16 octahedral sites. The M^{2+} cations (e.g. M^{2+} = Mg^{2+}, Mn^{2+}, Zn^{2+}, Ni^{2+}, Co^{2+}, Fe^{2+}, Cd^{2+} and Cu^{2+}) and Fe^{3+} cations balance between the tetrahedral and octahedral sites make three different spinel ferrite structure. If M^{2+} cations are situated at tetrahedral sites and Fe^{3+} cations are situated at octahedral sites, this type of structure is known as a normal spinel structure. If M^{2+} cations are situated at octahedral sites and Fe^{3+} cations are equally distributed between octahedral sites and tetrahedral sites, this type of structure is known as an inverse spinel structure. If M^{2+} and Fe^{3+} randomly occupy both tetrahedral and octahedral sites, this type of structure is known as a mixed spinel structure.[1,2] The nanomagnetic magnesium ferrite is widely used in various technological applications i.e. electrochemical sensor,[3] supercapacitors,[4] hyperthermia,[5] cobalt iron removal from synthetic wastewater,[6] anode material for lithium battery,[7] photodegradation of malachite green,[8] LPG sensor,[9] degradations of reactive blue dye.[10] Magnesium ferrite is a magnetic bi-oxide ceramic material with a partially inverse spinel structure. The distribution of the cations in magnesium ferrite can be represented by $(Mg^{2+}_{1-x}Fe^{3+}_{x})_A[Mg^{2+}_{x}Fe^{3+}_{2-x}]_BO^{2-}_4$ where *x* represents the degree of inversion of the cation in the structure.[11]

Several methods have been developed to synthesize nanomagnetic magnesium ferrite such as ultrasonic wave-assisted aqueous solution ball milling,[12] co-precipitation,[13] green syntheses,[14] hydrothermal decompositions,[15] supercritical hydrothermal reactions,[16] micro-emulsion methods,[17] oxalate co-precipitation,[18] reverse micelle processing,[19] starch-gel processes,[20] electrospinning.[21] In the present work, $MgFe_2O_4$ (MGF) ferrite nanoparticles have been synthesized through the auto combustion technique, and various physical properties like XRD, FTIR, EDAX, SEM, and magnetic measurements studied.

EXPERIMENTAL

To prepare nanomagnetic ferrites, $Mg(NO_3)_2{\cdot}6H_2O$ (0.5 mol, Merck, ACS) and $Fe(NO_3)_3{\cdot}9H_2O$ (1 mol, Merck, ACS) was dissolved in 50 ml water initially. The citric acid (1.11 mol, Merck, ACS) was used as a fuel for the auto combustion technique. The molar ratio was calculated according to the principle of propellant chemistry.[22] Citric acid dropwise added into the mixture of magnesium nitrate and iron nitrate. The initial pH of this solution was ~ 2. Then the ammonia solution was added dropwise to adjust the pH ~ 9. Simultaneously, the mixture was stirred at 80 ºC constant temperature on a magnetic stirrer. After a certain time lapsed, the mixture became red viscous gel and magnesium ferrite nanoparticles were obtained. These nanoparticles were sintered at 500 ºC for 5 hrs in a muffle furnace to remove impurities.

To check the proportion of Mg, Fe, and O in nanomagnetic magnesium ferrite, EDAX analysis (Energy Dissipative Analysis of X-ray) was used. To observe the internal structure of magnesium ferrite, SEM was used. The physical parameters like lattice parameters, particle size, and magnesium ferrite crystal structure were obtained by X-ray diffraction (XRD) characterization. The crystallite size was calculated by the Debye-Scherer formula using the highest peak (311) of XRD of prepared nano ferrite. The force constants between metal-oxygen were calculated using FTIR

spectroscopy. The prepared nano ferrite's magnetic properties have been studied at room temperature by means of hysteresis loop measurement using a vibrating sample magnetometer. Values of saturation magnetization and coercive field were obtained from the same. The cation distribution of prepared nano ferrite is obtained from the Mossbauer spectroscopy.

RESULT AND DISCUSSION

The EDAX analysis is performed to monitor the prepared sample's average elemental composition and confirm the purity. Figure 1 shows the EDAX pattern of the prepared sample that confirmed the presence of magnesium, iron, oxygen, and there are no other peaks for impurities.

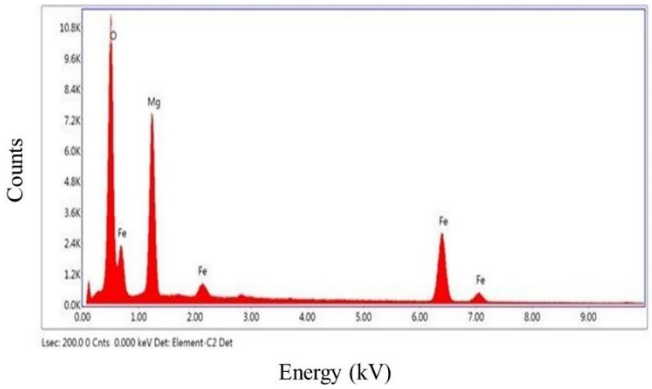

Figure 1. EDAX of $MgFe_2O_4$

Figure 2 shows the SEM image, which indicates the grains of ferrite are nanosized. Figure 3 indicates the pores, voids, and fractured surfaces that occur due to a large amount of toxic gas escaping during the combustion process.

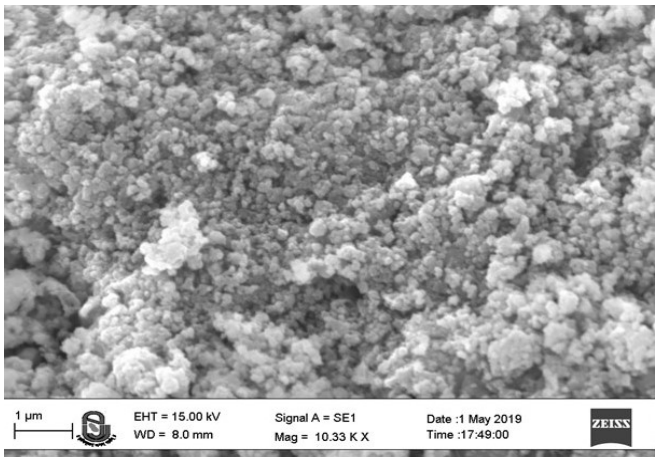

Figure 2. SEM image of grain size for $MgFe_2O_4$

The synthesized sample is subject to X-ray diffraction analysis at 300 K to identify phase and approximate crystallite size. Figure 4 shows the X-ray diffraction pattern of $MgFe_2O_4$. The $MgFe_2O_4$ spinel ferrite was indexed for the *fcc-Fd3m* space group using a standard data file obtained from the PCPDFWIN program (JCPDS card number: 73-2410).

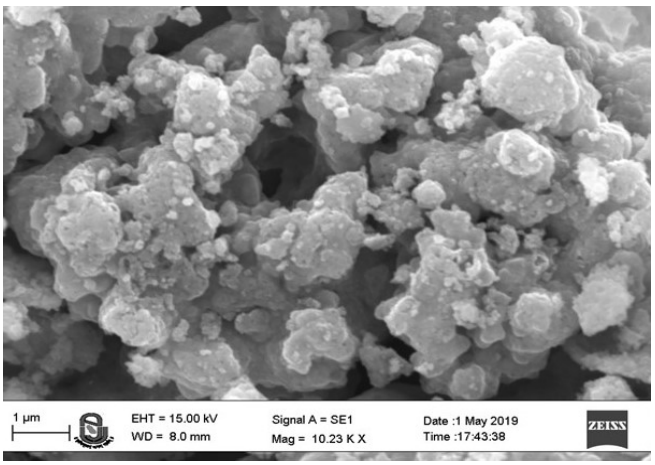

Figure 3. Surface morphology for $MgFe_2O_4$

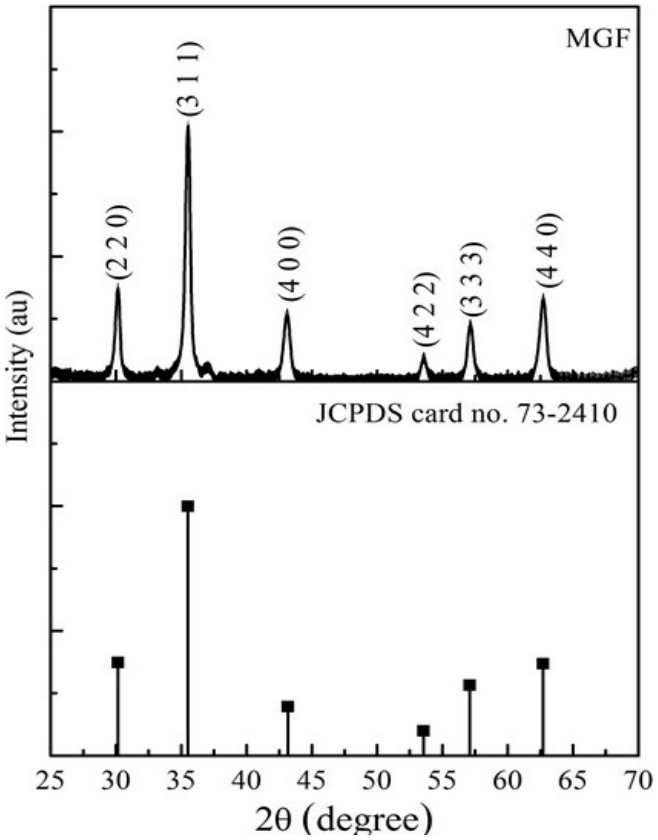

Figure 4. XRD pattern of $MgFe_2O_4$

MGF's crystallite size is calculated using the Debye-Scherrer formula by sharp Bragg reflection corresponding to an intense peak (311) about 15 nm. The synthesized spinel ferrite is subjected to a particle size analyzer and obtained an average crystallite size of 12.53 nm, as shown in Figure 5.

FTIR spectroscopy is generally used to determine the molecular and chemical structure of spinel ferrite. Two strong assigned absorption bands appear υ_1 (around 600 cm^{-1}) due to tetrahedrally coordinated metal ions and υ_2 (around 400 cm^{-1}) is due to octahedrally coordinated metal ions for spinel ferrite.[23]

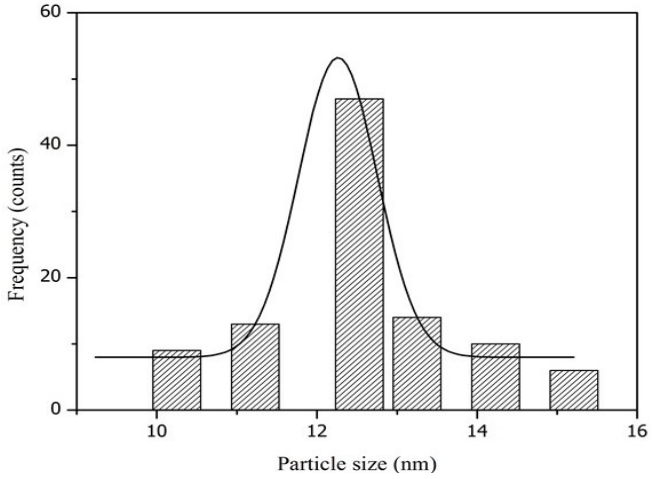

Figure 5. Particle size distribution of $MgFe_2O_4$

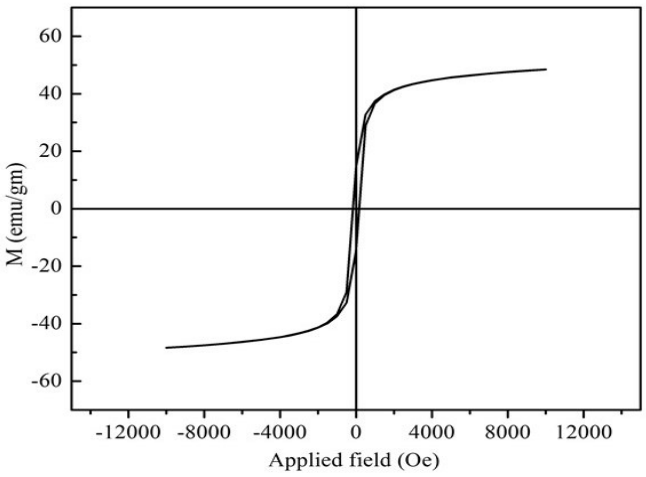

Figure 7. Hysteresis loop of $MgFe_2O_4$

In the present case, the IR absorption band appears at υ_1 = 678.97 cm^{-1} due to tetrahedral stretching vibrational mode ($O–M_{Tet}$) and υ_1 = 459.13 cm^{-1} due to octahedral stretching vibration mode($O–M_{Oct}$) of $MgFe_2O_4$ as shown in Figure 6. The Fourier Transform Infrared Spectrum of $MgFe_2O_4$ is recorded at 300 K in the range of 400 – 800 cm^{-1}. The force constant can be calculated for the tetrahedral site (k_t) = 181.65 N/m and octahedral site (k_o) = 94.82 N/m using the standard formulae the IR absorption spectra.[24]

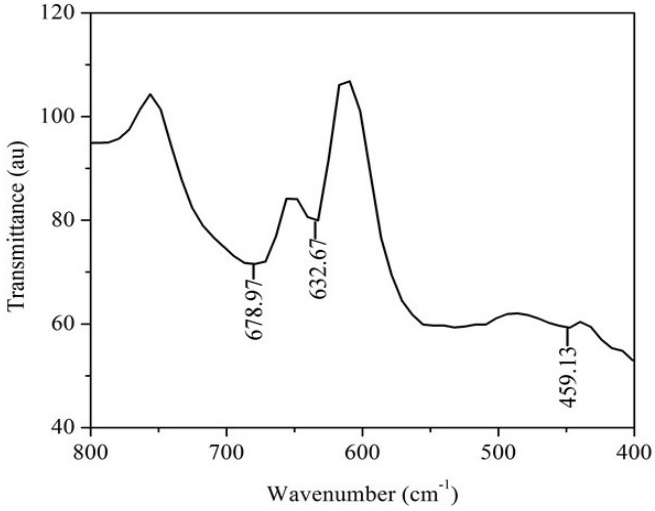

Figure 6. FTIR of $MgFe_2O_4$

Magnetic properties of $MgFe_2O_4$ are studied with the help of a vibrating sample magnetometer at room temperature at a maximum field of 10 kOe. The hysteresis curve of magnesium ferrite is shown in Figure 7. The magnesium ferrite shows ferromagnetic behavior with saturation magnetization (M_s) 48.4 emu g^{-1}, a coercivity of about 169.25 Oe, and remanence magnetization (M_r) 14.47 emu g^{-1}.

The magnetic energy of the ferrite particle is comparable to the thermal energy at room temperature. The broad doublet is fitted with two sets of doublets corresponding to quadrupole splitting (QS) in the iron nucleus in the shell and the shell's core region.[25-26]

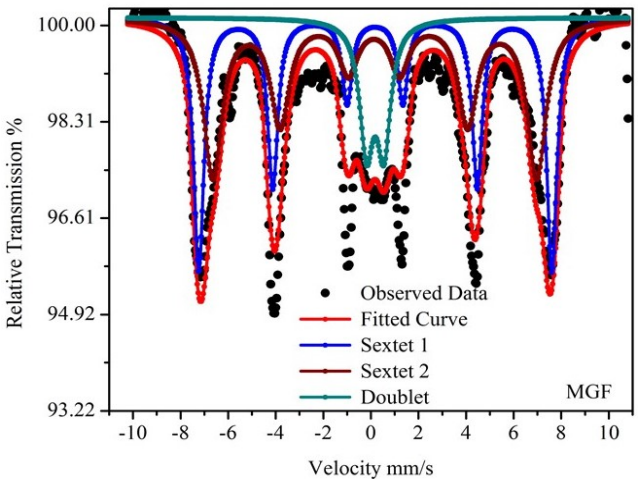

Figure 8. Mossbauer spectrum of $MgFe_2O_4$

Table 1. shows various parameters of the Mossbauer spectrum of $MgFe_2O_4$. Mossbauer results show that the cation distribution of $MgFe_2O_4$ would be $(Mg^{2+}_{1-x}Fe^{3+}_{x})_A[Mg^{2+}_{x}Fe^{3+}_{2-x}]_BO^{2-}_4$ where ions are enclosed by the parentheses correspond to the tetrahedral (A) site and the ions enclosed by the brackets correspond to the octahedral (B) site.[27] The ratio of Line width S1 to D1 was found to be 0.54, which is the value of x. The cation distribution found to be $(Mg^{2+}_{0.46}Fe^{3+}_{0.54})_A[Mg^{2+}_{0.54}Fe^{3+}_{1.46}]_BO^{2-}_4$.

Table 1. Mossbauer parameters of $MgFe_2O_4$

Sample	Sub spectrum	Line width, mm s^{-1}	IS 'δ', mm s^{-1}	Q splitting	Hyperfine field 'H_f', T	Area, %
MGF	S1	0.31	0.18	0.03	40.07	90.97
	D1	0.57	0.20	0.58	----	9.03

CONCLUSION

Magnesium ferrite nanoparticles are successfully synthesized by the auto combustion technique. Elemental analysis is shown through EDAX measurement. The X-ray diffraction study shows the formation of spinel structure. To validate the structure of the sample, FTIR spectra are recorded and force constants are calculated for the interstitial sites of the spinel ferrites. The crystallite size of nano-ferrites is calculated from the Debye-Scherrer equation using the intense peak of XRD and the particle size analyzer confirms the crystallite size of the prepared sample. The superparamagnetic nature of the nano magnesium ferrite is evaluated through VSM analysis and the presence of doublet in Mossbauer spectra supports the same. The cation distribution of the $MgFe_2O_4$ is established through the Mossbauer spectroscopy.

REFERENCES

[1]Šutka, A., Gross, K. A., Spinel ferrite oxide semiconductor gas sensors, *Sensors Actuators B, Chem.*, **2016**, *222*, 95–105. DOI: 10.1016/j.snb.2015.08.027.

[2]Tanna, A. R.and Joshi, H. H., Computer-Aided X-Ray Diffraction Intensity Analysis for Spinels : Hands-On Computing Experience, *Int. J. Math., Phys., Elect. Comp. Engg.*, **2013**, *7(3)*, 334–341.

[3]Ensafi, A. A., Allafchian, A. R., Mohammadzadeh, R., Characterization of $MgFe_2O_4$ Nanoparticles as a Novel Electrochemical Sensor: Application for the Voltammetric Determination of Ciprofloxacin, *Anal. Sci.*, **2012**, *28(7)*, 705–710. DOI: 10.2116/analsci.28.705.

[4]Malaie, K., Ganjali, M. R., Alizadeh, T., Norouzi, P., Hydrothermal growth of magnesium ferrite rose nanoflowers on Nickel foam; application in high-performance asymmetric supercapacitors, *J. Mater. Sci. Mater. Electron.*, **2018**, *29(01)*, 650–657. DOI: 10.1007/s10854-017-7958-3.

[5]Khot, V. M., Salunkhe, A. B., Thorat, N. D., Phadatare, M. R., Pawar, S. H., Induction heating studies of combustion synthesized $MgFe_2O_4$ nanoparticles for hyperthermia applications, *J. Magn. Magn. Mater.*, **2013**, *33(7407)*, 48–51. DOI: 10.1016/j.jmmm.2012.12.010.

[6]Srivastava, V., Sharma, Y. C., Sillanpää, M., Application of nano-magneto ferrite (n-$MgFe_2O_4$) for the removal of Co^{2+} ions from synthetic wastewater: Kinetic, equilibrium and thermodynamic studies *Appl. Surf. Sci.*, **2015**, *338*, 42–54. DOI: 10.1016/j.apsusc.2015.02.072.

[7]Narsimulu, D., Rao, B. N., Venkateswarlu, M., Srinadhu, E. S. and Satyanarayana, N., Electrical and electrochemical studies of nanocrystalline mesoporous $MgFe_2O_4$ as anode material for lithium battery applications, *Ceram. Int.*, **2016**, *42 (15)*, 16789–16797. DOI: 10.1016/j.ceramint.2016.07.168.

[8]Saeid, S. G., Fardood, T., Moradnia, F., Mostafaei, M., Afshari, Z., Faramarzi, V., Biosynthesis of $MgFe_2O_4$ magnetic nanoparticles and their application in photodegradation of malachite green dye and kinetic study, *Nanochem. Res.*, **2019**, *4(1)*, 86–93. DOI: 10.22036/ncr.2019.01.010.

[9]Patil, J. Y., Khandekar, M. S., Mulla, I. S., Suryavanshi, S. S., Combustion synthesis of magnesium ferrite as liquid petroleum gas (LPG) sensor: Effect of sintering temperature, *Curr. Appl. Phys.*, **2012**, *12(1)*, 319–324. DOI: 10.1016/j.cap.2011.06.029.

[10]Fardood S. T., Golfar, Z., Ramazani, A. *J.*, Novel sol-gel synthesis and characterization of superparamagnetic magnesium ferrite nanoparticles using tragacanth gum as a magnetically separable photocatalyst for degradation of reactive blue 21 dye and kinetic study, *Mater. Sci. Mater. Electron.*, **2017** DOI: 10.1007/s10854-017-7622.

[11]Naseri, M. G., Ara, M. H. M., Saion, E. B., Shaari, A. H., Superparamagnetic magnesium ferrite nanoparticles fabricated by a simple, thermal-treatment method, *J. Magn. Magn. Mater.*, **2014,** *350*, 141–147. DOI: 10.1016/j.jmmm.2013.08.032.

[12]Chen, D., Li, D. Y., Zhang, Y. Z., Kang, Z. T., Preparation of magnesium ferrite nanoparticles by ultrasonic wave-assisted aqueous solution ball milling, *Ultrason. Sonochem*, **2013,** *20(6)*, 1337–1340. DOI: 10.1016/j.ultsonch.2013.04.001.

[13]Thankachan, S., Xavier, S., Jacob, B., Mohammed, E. M. *J.*, A comparative study of structural, electrical and magnetic properties of magnesium ferrite nanoparticles synthesised by sol-gel and co-precipitation techniques, *Exp. Nanosci.*, **2013,** *8(3)*, 347–357. DOI: 10.1080/17458080.2012.690892.

[14]Joulaei, M., Hedayati, K., Ghanbari, D., Investigation of magnetic, mechanical and flame retardant properties of polymeric nanocomposites: Green synthesis of $MgFe_2O_4$ by lime and orange extracts, *Compos. Part B Eng.*, **2019**, *176*, 107345. DOI: 10.1016/j.compositesb.2019.107345.

[15]Ilhan, S., Izotova, S. G., Komlev, A. A., Synthesis and characterization of $MgFe_2O_4$ nanoparticles prepared by hydrothermal decomposition of co-precipitated magnesium and iron hydroxides, *Ceram. Int.*, **2015**, *41(1)*, 577–585. DOI: 10.1016/j.ceramint.2014.08.106.

[16]Sasaki, T., Ohara., S., Naka, T., Vejpravova, J., Sechovsky, V., Umetsu, M., Takami, S., Jeyadevan, B., Adschiri, T., Continuous synthesis of fine $MgFe_2O_4$ nanoparticles by supercritical hydrothermal reaction, *J. Supercrit. Fluids*, **2010**, *53(1-3)*,92–94. DOI: 10.1016/j.supflu.2009.11.005

[17]Ali, R., Khan, M. A., Mahmood, A., Chughtai, A. H., Sultan, A., Shahid, M., Ishaq, M.,Warsi, M. F., Structural, magnetic and dielectric behavior of $Mg_{1-x}Ca_xNi_yFe_{2-y}O_4$ nano-ferrites synthesized by the micro-emulsion method, *Ceram. Int.*, **2014**, *40(03)*, 3841–3846. DOI: 10.1016/j.ceramint.2013.08.024.

[18]Shedam, R. M., Gadkari, A. B., Mathad, S. N., Shedam, M. R., Structural and mechanical properties of nano grained magnesium ferrite produced by oxalate co-precipitation method, *Int. J. Self-Propagating High-Temperature Synth.*, **2017**, *26(1)*, 75–79. DOI: 10.3103/S1061386217010113.

[19]Chandradass, J., Kim, K. H., Solvent effects in the synthesis of $MgFe_2O_4$ nanopowders by reverse micelle processing, *J. Alloys Compd.*, **2011**, *509(5)*,59–62. DOI: 10.1016/j.jallcom.2010.10.090.

[20]Köferstein, R., Walther, T., Hesse, D., Ebbinghaus, S. G., Preparation and characterization of nanosized magnesium ferrite powders by a starch-gel process and corresponding ceramics, *J. Mater. Sci.*, **2013**, *48(19)*, 6509–6518. DOI: 10.1007/s10853-013-7447-x.

[21]Maensiri, S., Sangmanee, M., Wiengmoon, A., Magnesium ferrite ($MgFe_2O_4$) nanostructures fabricated by electrospinning, *Nanoscale Res. Lett.*,**2009**. DOI: 10.1007/s11671-008-9229-y.

[22]Sutka, A., Mezinskis, G., Sol-gel auto-combustion synthesis of spinel-type ferrite nanomaterials, *Front. Mater. Sci.*, **2012,** *6(2)*, 128–141. DOI: 10.1007/s11706-012-0167-3

[23]Waldron, R. D., *Infrared Spectra of Ferrites, Phys. Rev.*, **1955**, *99(6)*, 1727-1735.

[24]Thummer, K. P., Tanna, A. R., Joshi, H. H., Rietveld structure refinement and elastic properties of $MgAl_xCr_xFe_{2-2x}O_4$ spinel ferrites, *AIP Conf. Proc.*, **2017**, *(1837)*, 1–5. DOI: 10.1063/1.4982142.

[25]Rangolia, M. K., Chhantbar, M. C., Tanna, A. R., Modi, K. B., Baldha, G. J., Joshi, H. H., Magnetic behavior of nanosized and coarse powders of Cd-Ni ferrites synthesized by wet-chemical route, *Ind. J. Pure Appl. Phys.*, **2008,** *46*, 60–64.

[26]Tanna, A. R., Sosa, K. M., Joshi, H. H., Study of superparamagnetic nanoparticles of $Mn_xCo_{1-x}Fe_2O_4$ ferrite system prepared by co-precipitation technique *Mater. Res. Express*, **2017**, *4(11)*. DOI: 10.1088/2053-1591/aa9393.

[27]Kulkarni, R. G., Joshi, H. H., Comparison of Magnetic Properties of $MgFe_20_4$ Prepared by Wet-Chemical and Ceramic Methods *J. Solid. State Chem.*, **1986**, *147*, 141–147. DOI:10.1016/0022-4596(86)90133-7.

This paper was presented at the International Conference "

CONFERENCE ON MOLECULAR STRUCTURE & INSTRUMENTAL APPROACHES"

at RK University, Rajkot (Gujarat-India) on 26-27th November 2020

Received: 14.12.2020.
Accepted: 22.01.2021.